European Radiology (2019) 29:3761–3771
https://doi.org/10.1007/s00330-019-06052-8

GASTROINTESTINAL

Hepatic sarcomatoid carcinoma: magnetic resonance imaging evaluation by using the liver imaging reporting and data system

Nieun Seo[1] · Myeong-Jin Kim[1] · Hyungjin Rhee[1]

Received: 6 November 2018 / Revised: 21 December 2018 / Accepted: 30 January 2019 / Published online: 11 March 2019

Abstract

Objectives To evaluate how sarcomatoid carcinomas (SCs) would be classified on magnetic resonance imaging (MRI) by using the Liver Imaging Reporting and Data System (LI-RADS) and to assess imaging features of SC compared with other hepatic malignancies.

Methods We retrieved 184 patients with pathologically confirmed SC ($n = 46$), hepatocellular carcinoma (HCC, $n = 92$), and intrahepatic cholangiocarcinoma (iCCA, $n = 46$) diagnosed between January 2006 and December 2017. Two readers independently reviewed MRI according to LI-RADS v2017. Classification rate of SC, as probably or definitely malignant but not specific for HCC (LR-M), was calculated. LR-TIV (tumor in vein) was subclassified as either 5V or MV. MRI features were compared between SC, HCC, and iCCA and between SC of LR-M and non-LR-M categories.

Results Chronic liver disease was present in 71.7% (33/46) of patients with SC, and LI-RADS was applied for these patients. SC was classified as LR-M in 24 (72.7%) of 33 patients at risk. SCs that had been classified as LR-4/5/5V were significantly smaller (median, 1.9 cm; range, 1.0–4.2 cm) than SCs classified as LR-M/MV (median, 4.3 cm; range, 1.3–20.6 cm) on independent *t* test ($p = 0.012$). SCs commonly showed MRI features similar to iCCAs than to HCCs. Targetoid appearance and capsular retraction were more frequent in iCCA than in SC ($p \leq 0.009$) on Pearson's chi-squared test or Fisher's exact test.

Conclusion Most SCs can be classified as LR-M on MRI, but small lesions may be indistinguishable from HCCs.

Key Points

- *Most sarcomatoid carcinomas (SCs) are classified as LR-M on MRI by using LI-RADS v2017.*
- *SC showed various LR-M features similar to those of intrahepatic cholangiocarcinoma.*
- *Size of LR-4/5/5V SC was significantly smaller than that of LR-M/MV SC.*

Keywords Hepatocellular carcinoma · Cholangiocarcinoma · Magnetic resonance imaging · Liver neoplasms

Abbreviations

CLD	Chronic liver disease
DWI	Diffusion-weighted imaging
HBP	Hepatobiliary phase
HCC	Hepatocellular carcinoma
iCCA	Intrahepatic cholangiocarcinoma
LI-RADS	Liver Imaging Reporting and Data System
MRI	Magnetic resonance imaging
SC	Sarcomatoid carcinoma
T1WI	T1-weighted imaging
T2WI	T2-weighted imaging
TIV	Tumor in vein

✉ Myeong-Jin Kim
kimnex@yuhs.ac

[1] Department of Radiology, Research Institute of Radiological Science, Severance Hospital, Yonsei University College of Medicine, 50-1 Yonsei-ro, Seodaemun-gu, Seoul 03722, South Korea

Introduction

Hepatic sarcomatoid carcinoma (SC) is a rare malignant hepatic tumor comprising carcinomatous and sarcomatous components [1, 2]. SC may be subclassified as sarcomatoid hepatocellular carcinoma (S-HCC), sarcomatoid intrahepatic cholangiocarcinoma (S-iCCA), or undifferentiated carcinoma according to the main carcinomatous component [3]. The prognosis of SC is known to be poor, due to more advanced histologic grades and a higher rate of recurrence or metastasis

than in ordinary hepatocellular carcinoma (HCC) or ordinary intrahepatic cholangiocarcinoma (iCCA) [1, 4–8]. Therefore, identifying SC is important for proper patient management and treatment planning.

Few studies have reported the imaging findings of hepatic SC [9–13]. SCs tend to appear as large intrahepatic masses with peripheral enhancement, large area of central necrosis, and frequent intrahepatic metastases and tumor seeding on computed tomography or magnetic resonance imaging (MRI) [9–14]. These findings may help distinguish SC from HCC, but may mimic other hepatic malignancies like iCCA. Moreover, no controlled studies have compared the imaging findings between SC and HCC or iCCA.

The Liver Imaging Reporting and Data System (LI-RADS) is a comprehensive system for standardized interpretation and reporting of imaging in patients at high risk of developing HCC [15]. Unlike other guidelines for HCC diagnosis [16, 17], the LI-RADS includes a category for lesions that are probably or definitely malignant, but not specific for HCC (LR-M), in addition to categories reflecting the probability of HCC (LR-1–5). It might be desirable that hepatic SC should be classified as LR-M, in order to avoid being diagnosed as HCC by imaging criteria alone and then undergoes treatment without histologic diagnosis. However, to our knowledge, no study has evaluated the imaging features of SC by using the LI-RADS.

Therefore, we aimed to evaluate how SC would be classified on MRI when using the LI-RADS and to assess imaging features of SC compared with those in other primary hepatic malignancies.

Materials and methods

Patients

This retrospective study was approved by our institutional review board, which waived the requirement for informed consent. We searched our electronic medical records for patients with pathologically proven liver tumors diagnosed between January 2006 and December 2017, by using the search terms “sarcomatoid” or “sarcomatous.” Of 6901 patients with pathologically proven malignant hepatic tumors, 79 had hepatic SCs. Among these, 33 were excluded because of (a) no liver MRI ($n = 14$), (b) non-hepatic primary SC ($n = 6$), and (c) treated hepatic SC prior to liver MRI ($n = 13$). Finally, 46 patients with hepatic SCs were included. The SC subtypes were sarcomatoid HCC (S-HCC, $n = 17$), sarcomatoid iCCA (S-iCCA, $n = 13$), sarcomatoid combined HCC and cholangiocarcinoma (S-cHCC-CC, $n = 7$), and undifferentiated SC (u-SC, $n = 9$). Undetermined SCs were confirmed by liver biopsy, which limited further classification of specific histologic types. For selecting patients with HCC or iCCAs over the same period and for comparison of their clinical and MRI features to those of patients with SCs, 1:2 and 1:1 propensity score matching was used respectively. Finally, 46 patients with SCs, 92 with HCCs, and 46 with iCCAs were included (M:F, 141:43; mean age ± standard deviation, 61.2 ± 10.5 years; Fig. 1). The sex ratio was comparable between the three groups, which reflected the prevalence in general population. Of these 184 patients, 123 had underlying chronic liver disease (CLD), with the following etiology: hepatitis B virus ($n = 100$), hepatitis C virus ($n = 9$), alcoholic liver disease ($n = 8$), and others ($n = 6$). Regarding the type of reference standard, 53.8% (99/184) of patients underwent hepatic resection and 46.2% (85/184) underwent percutaneous liver biopsy.

MR image acquisition

Liver MRI was performed using a 3.0-T (MAGNETOM Tim Trio, Siemens Healthineers; Intera Achieva, Philips Healthcare) or a 1.5-T system (Intera Achieva, Philips Healthcare). Our routine liver MRI protocol included dual-echo spoiled gradient-echo T1-weighted in-phase and opposed-phase imaging, multi-shot and single-shot turbo spin-echo T2-weighted imaging (T2WI), and dynamic T1-weighted imaging (T1WI). Single-shot echo planar diffusion-weighted imaging (DWI) was performed using b values of 50, 400, and 800 s/mm^2. Dynamic fat-suppressed spoiled gradient-echo T1WI was acquired before and after contrast injection: gadoxetate disodium (Primovist®, Bayer Pharma AG) in 114 patients, gadobenate dimeglumine (MultiHance®, Bracco SPA) in 6, gadoterate meglumine (Dotarem®, Guerbet SA) in 60, and gadopentetate dimeglumine (Magnevist®, Bayer Pharma AG) in 4. Gadoxetate disodium was administered at a dose of 0.1 mL/kg (0.025 mmol/kg) followed by a 20-mL saline flush at an injection rate of 1 mL/s. Other contrast agents were injected at a dose of 0.1 mmol/kg, followed by a 20-mL saline flush at an injection rate of 2 mL/s. To determine the optimal timing of the arterial phase, a test bolus technique or bolus-tracking method was used. Subsequent dynamic phases were acquired with intervals of approximately 30 s; each dynamic phase required 16–22 s. The hepatobiliary phase (HBP) was obtained 15–20 min after gadoxetate disodium injection and 2 h after gadobenate dimeglumine injection. Among the 184 patients, 64 patients who had MRI with extracellular contrast agents had no HBP data, and seven patients had no available DWI data, respectively.

Image analysis

Two abdominal radiologists, with 25 or 5 years of experience in liver imaging, independently reviewed the MR images. For LI-RADS categorization and review of all MRI features, any discrepancy between the reviewers was resolved by consensus

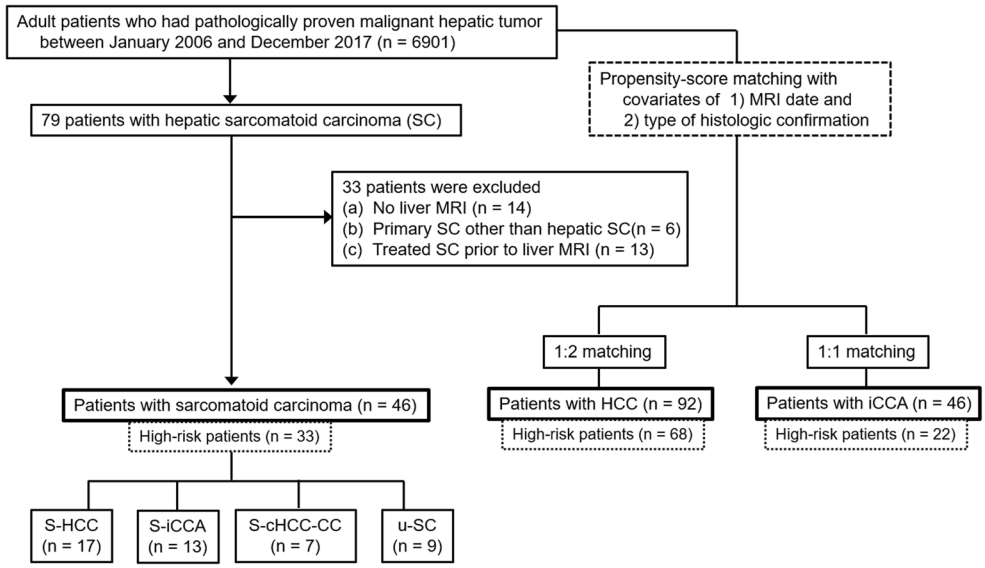

Fig. 1 Patient enrollment process. High-risk patients are those who had underlying chronic liver disease. MRI, magnetic resonance imaging; SC, sarcomatoid carcinoma; HCC, hepatocellular carcinoma; iCCA, intrahepatic cholangiocarcinoma; S-HCC, sarcomatoid hepatocellular carcinoma; S-iCCA, sarcomatoid intrahepatic cholangiocarcinoma; S-cHCC-CC, sarcomatoid combined hepatocellular and cholangiocarcinoma; u-SC, undifferentiated sarcomatoid carcinoma

review, and consensus data were used for analysis. The reviewers were aware that all the patients had pathologically confirmed primary hepatic malignancy, but were blinded to the specific histopathological diagnosis or other clinical findings. Prior to image review, the size and location of the tumor were provided via series/image numbers and arrows on the picture archiving and communication system by a study coordinator (an abdominal radiologist with 5 years of experience in liver imaging) who did not participate in the image review. If the patients had multiple hepatic tumors, the largest representative lesion was considered the index lesion. The largest diameter of the tumor was measured in the phase in which the lesion was best demarcated [18].

For 123 patients with risk factors, reviewers assigned LI-RADS categories (LR-1–5 or LR-M) to the tumors by using major and ancillary features of LI-RADS v2017. LR-TIV (tumor in vein) was assigned when unequivocal soft tissue in vein was present, regardless of parenchymal mass. If the parenchymal mass was present in LR-TIV cases, LR-TIV was subclassified according to imaging features of the associated parenchymal mass, such as LR-5V or LR-MV.

Additionally, reviewers evaluated the following MRI features in all 184 patients: (a) tumor shape (round, lobulated, or irregular/geographic); (b) enhancement pattern; (c) enhancing and nonenhancing capsule; (d) signal intensity of the tumor relative to liver parenchyma on T2WI, DWI, and HBP; (e) targetoid appearance on DWI and HBP; (f) TIV; (g) other ancillary features; and (h) additional imaging features. Enhancement patterns included arterial-phase hyperenhancement (no, rim-like, or non-rim-like) and washout (no, peripheral, non-peripheral). Washout appearance was defined in the portal venous phase on gadoxetate-enhanced MRI, and in the portal venous and delayed phases on MRI using extracellular contrast agents. Delayed central enhancement (defined as a central area of progressive postarterial-phase enhancement) [15] was also assessed. Capsule appearance was considered present when it appeared around at least two-thirds of the tumor border [19]. T2WI was also evaluated for intralesional bright signal intensity, which was higher than that of the spleen, suggesting intratumoral necrosis. Other ancillary features included intralesional fat or hemorrhage and mosaic appearance. We also evaluated additional imaging features other than LI-RADS including capsular retraction, adjacent biliary dilatation, and intrahepatic and extrahepatic metastases. Intrahepatic metastasis was defined as a nodule having the same imaging characteristics as those in the main mass and being separated > 2 cm in distance from the main mass. The major and ancillary features were defined according to the LI-RADS v2017 [15].

Pathologic evaluation

Histologically, SCs comprised varying proportions of spindle cell components and carcinomatous components. The latter exhibited hepatocellular differentiation (S-HCC) or biliary differentiation (S-iCCA), or both (S-cHCC-CC). The differentiation status of tumors was primarily evaluated using hematoxylin-eosin staining; additionally, various histochemical stains, including mucicarmine and alcian blue/periodic acid-Schiff, and immunohistochemical markers, including cytokeratin (AE1/AE3), vimentin, HepPar1, arginase-1, alpha-fetoprotein, keratin 19, and polyclonal carcinoembryonic antigen, were applied as appropriate. The exact differentiation

of carcinomatous components could not be determined in some biopsied cases because of specimen limitations; therefore, such cases were classified as u-SCs.

Statistical analysis

To compare the clinical and MRI features between hepatic SCs and other primary hepatic malignancies, patients with HCCs and iCCAs were selected using 1:2 and 1:1 propensity score matching via the nearest-neighbor matching method. MRI date and type of histologic confirmation (operation or biopsy) were used as covariates to match the MRI scan protocols, including type of contrast agent, and to match the operability of tumors.

As the LI-RADS should be applied in patients at high risk of developing HCC, we calculated the sensitivity, specificity, and accuracy of LR-5/5V and LR-M/MV for patients at high risk only. Correct LI-RADS category of SCs was considered as LR-M. Sensitivity, specificity, and accuracy of LR-5/5V were used for the diagnosis of HCC, and those of LR-M/MV were applied for the diagnosis of non-HCC malignancy (iCCAs or SCs in this study). Interobserver agreement for LI-RADS categorization was assessed using κ statistics: κ values < 0.20, poor; 0.21–0.40, fair; 0.41–0.60, moderate; 0.61–0.80, good; and 0.81–1.00, excellent agreement. Normal distribution of the data was tested using the Kolmogorov-Smirnov test and Shapiro-Wilk test. Comparison of the clinical and MRI features among patients with SCs, HCCs, and iCCAs was performed using one-way analysis of variance with post hoc analysis and the Bonferroni correction for continuous variables, and Pearson's chi-squared test or Fisher's exact test for categorical variables. The corrected p values were calculated by multiplying the original p values by the number of comparisons. The clinical and MRI features of patients with SCs were compared between LR-M/MV and non-LR-M/MV by using independent t test for continuous variables and Pearson's chi-squared test or Fisher's exact test for categorical variables.

Statistical analyses were performed using R version 3.3.3 (R Foundation for Statistical Computing) and IBM SPSS Statistics, Version 23.0 (IBM Corp.). P values < 0.05 were considered statistically significant.

Results

LI-RADS categorization of hepatic SC, HCC, and iCCA

Among 46 patients with SCs, 33 patients had CLD. For 33 patients with SCs at risk of HCC, 24 (72.7%) were classified as LR-M (Table 1; Figs. 2 and 3). Six SCs were classified as LR-4 or 5 (Fig. 4), and three SCs were classified as LR-TIV (Fig. 5). Among the three LR-TIV cases, one was classified as LR-5V and two were classified as LR-MV, according to the associated parenchymal mass. There were no LR-TIV cases with no discernible parenchymal mass in this study. None of the SCs were classified as LR-1 to 3. Sensitivity, specificity, and accuracy of the LR-M/MV category for diagnosing non-HCC malignancy were 81.8%, 85.3%, and 83.7%, respectively, in patients at high risk of HCC (Table 2). In SC patients, the sensitivity of LR-M/MV for the diagnosis of SC was 78.8%. Interobserver agreement for LI-RADS categorization between both reviewers was good (κ, 0.659; 95% confidence interval, 0.554–0.764).

Table 1 LI-RADS categories of SC, HCC, and iCCA on magnetic resonance imaging in high-risk patients

	LR-4	LR-5	LR-M	LR-TIV
SC (n = 33)	2 (6.0)	4 (12.1)	24 (72.7)	3 (9.1)
S-HCC (n = 16)	2 (12.5)	3 (18.8)	10 (62.5)	1 (6.3)
S-iCCA (n = 7)	0 (0)	0 (0)	7 (100)	0 (0)
S-cHCC-CC (n = 7)	0 (0)	1 (14.3)	5 (71.4)	1 (14.3)
u-SC (n = 3)	0 (0)	0 (0)	2 (66.7)	1 (33.3)
HCC (n = 68)	2 (2.9)	49 (72.1)	7 (10.3)	10 (14.7)
iCCA (n = 22)	0 (0)	3 (13.6)	18 (81.8)	1 (4.5)

Data in parentheses are percentages. Percentages may not add up to 100% because of rounding

LI-RADS, Liver Imaging Reporting and Data System; *SC*, sarcomatoid carcinoma; *HCC*, hepatocellular carcinoma; *iCCA*, intrahepatic cholangiocarcinoma; *S-HCC*, sarcomatoid HCC; *S-iCCA*, sarcomatoid iCCA; *S-cHCC-CC*, sarcomatoid combined hepatocellular and cholangiocarcinoma; *u-SC*, undifferentiated sarcomatoid carcinoma

Features of hepatic SC compared with those of HCC and iCCA

The incidence of CLD was 71.7% in patients with SC, 73.9% in those with HCC, and 47.8% in those with iCCA without significant differences between SC and HCC ($p > 0.999$), and SC and iCCA ($p = 0.057$; Table 3). On liver MRI, SCs showed lobulated or irregular shapes more frequently than did HCCs (83.1% vs. 54.3%, $p = 0.009$). SCs showed the following features less frequently than did HCCs: non-rim-like arterial enhancement, non-peripheral washout, enhancing and nonenhancing capsules, and mosaic appearance ($p \leq 0.027$). Delayed central enhancement, targetoid appearance on DWI or HBP, adjacent biliary dilatation, and extrahepatic metastasis were more frequent in SC than in HCC ($p \leq 0.030$). Targetoid appearance on DWI or HBP and capsular retraction were more frequent in iCCA than in SC ($p \leq 0.009$).

Features of hepatic SC: comparison between the LR-M/MV and LR-4/5/5V categories

Patients with SC classified as LR-M/MV were older than those with SC classified as LR-4/5/5V ($p = 0.020$).

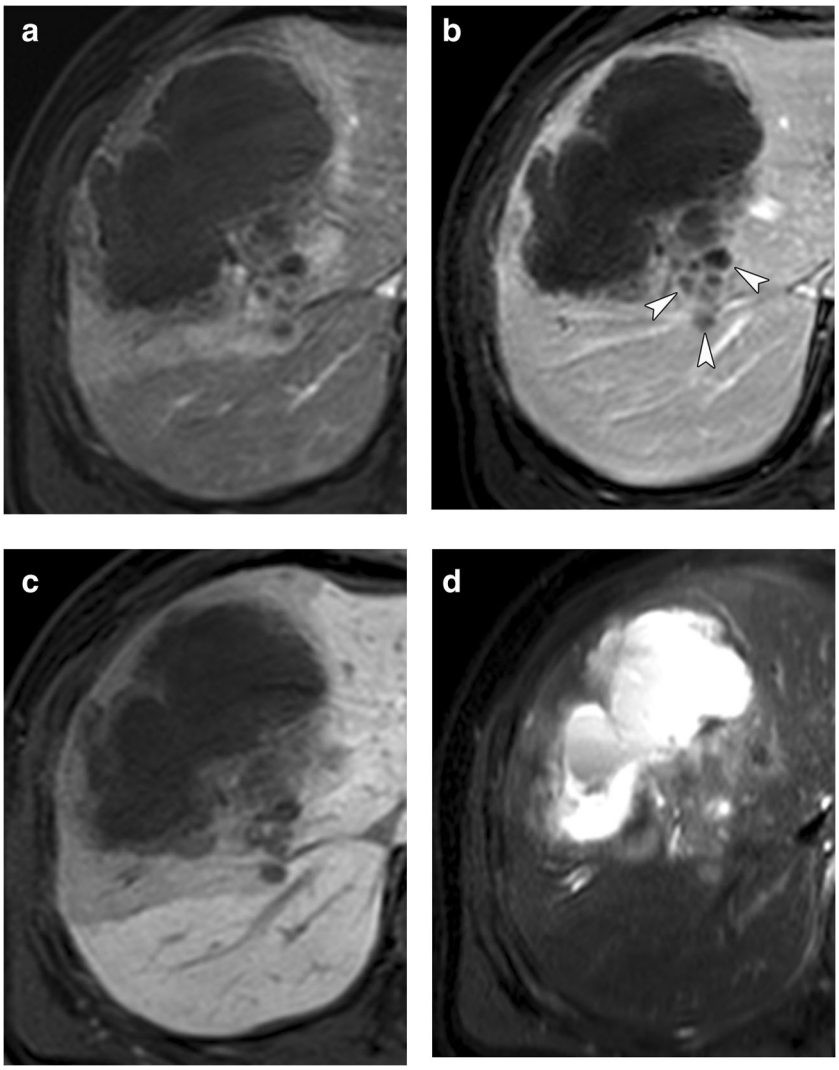

Fig. 2 A 10.2-cm sarcomatous intrahepatic cholangiocarcinoma of LR-M category in an 86-year-old man. Axial T1-weighted images acquired during the arterial (**a**), portal venous (**b**), and hepatobiliary (**c**) phases show a lobulated mass with poor enhancement and multiple intrahepatic metastases (arrowheads). **d** Axial T2-weighted image shows the tumor with a large central area of bright signal intensity, suggestive of necrosis

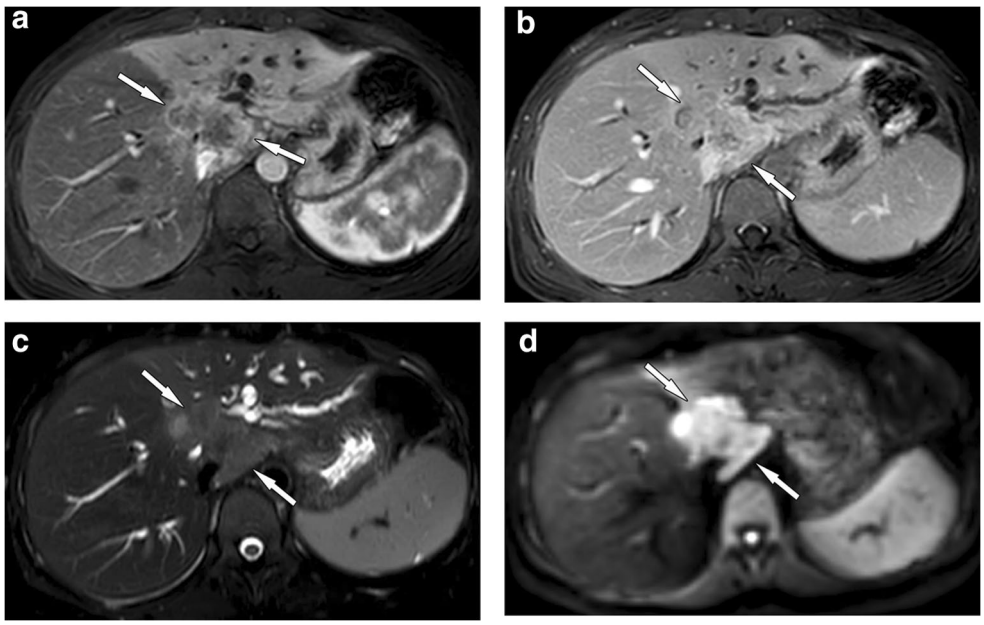

Fig. 3 A 5.2-cm undifferentiated sarcomatoid carcinoma of LR-M category in a 41-year-old woman. **a** Axial arterial-phase magnetic resonance (MR) image shows a lobulated mass with peripheral enhancement in the central liver. **b** Axial 3-min delayed-phase MR image shows gradual enhancement of the mass (arrows). **c** Axial T2-weighted image shows moderate hyperintensity of the mass with intrahepatic duct dilatation, which mimics intrahepatic cholangiocarcinoma. This mass shows diffusion restriction in the diffusion-weighted image (**d**) ($b = 800$ s/mm^2)

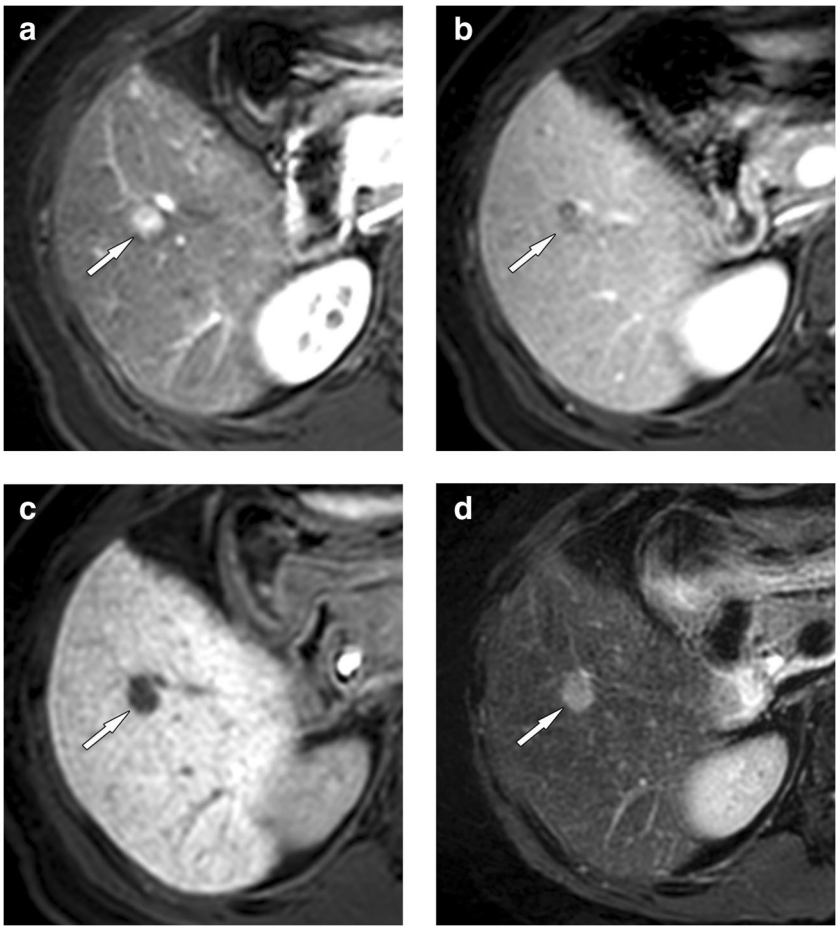

Fig. 4 A 1.3-cm sarcomatoid hepatocellular carcinoma of LR-4 category in a 49-year-old woman. Axial T1-weighted images acquired during the arterial (**a**) and portal venous (**b**) phases show a hepatic nodule (arrows) with homogeneous arterial hyperenhancement and washout appearance. **c** Axial hepatobiliary phase image shows avid hypointensity of the mass (arrow). **d** Axial T2-weighted image shows the tumor with moderate hyperintensity (arrow)

Histological subtypes of LR-4/5/5V SC were S-HCC in five patients and S-cHCC-CC in two (Table 4). Tumor size was significantly smaller in LR-4/5/5V SC than in LR-M/MV SC ($p = 0.012$). LR-4/5/5V SCs showed a higher frequency of imaging features that favored HCCs ($p \leq 0.040$), and a lower frequency of intrahepatic metastasis ($p = 0.032$; Figs. 4 and 5).

Discussion

We investigated the imaging features of SC by using the LI-RADS v2017 on MRI. Most SCs were classified as LR-M (24/33, 72.7%). SCs classified as LR-4/5 were encountered in S-HCC and S-cHCC-CC, but not in S-iCCA or u-SC. Thus, the MRI findings of SC might have reflected its dominant carcinomatous component. However, subgroup analysis could not be performed because of the small sample size. The tumor size of LR-4/5/5V SC was significantly smaller than that of LR-M/MV, as noted in previous studies on iCCA [20–22], suggesting SC may mimic HCC when they are small: All LR-4/5/5V SCs (7/7) were deemed to show non-rim arterial enhancement and washout enhancement patterns. Conventional capsule and mosaic appearance were also present in 57.1% (4/7) and 28.6% (2/7) of LR-4/5/5V SCs, respectively. Therefore, the occasional presence of these HCC features could hinder the differential diagnosis of some SCs from typical HCCs.

In our study, most patients with SCs had underlying CLD, similar to patients with HCCs (71.7% vs. 73.9%, $p > 0.999$). Previous studies also showed that 47.8–70.1% of patients with SC had cirrhosis or chronic hepatitis [2, 9]. Therefore, patients with SC may be a target population of LI-RADS categorization. In high-risk patients, 78.8% of SCs were classified as LR-M/MV. Given this high sensitivity for LR-M/MV, the LI-RADS would minimize the misdiagnosis of SC as HCC or benign lesions, thereby avoiding improper treatment such as liver transplantation or delayed management. For diagnosing non-HCC malignancies in patients at risk of HCC, LR-M/MV had a sensitivity, specificity, and accuracy of 81.8%, 85.3%, and 83.7%, respectively. The diagnostic performance of the LI-RADS in our study was also comparable to those in previous studies [23–25].

Our study also showed that SCs commonly present MRI findings similar to iCCAs than to HCCs, including lobulated shape, rim-like arterial-phase hyperenhancement, peripheral washout, delayed central enhancement, and biliary dilatation. Moreover, several imaging features characterizing

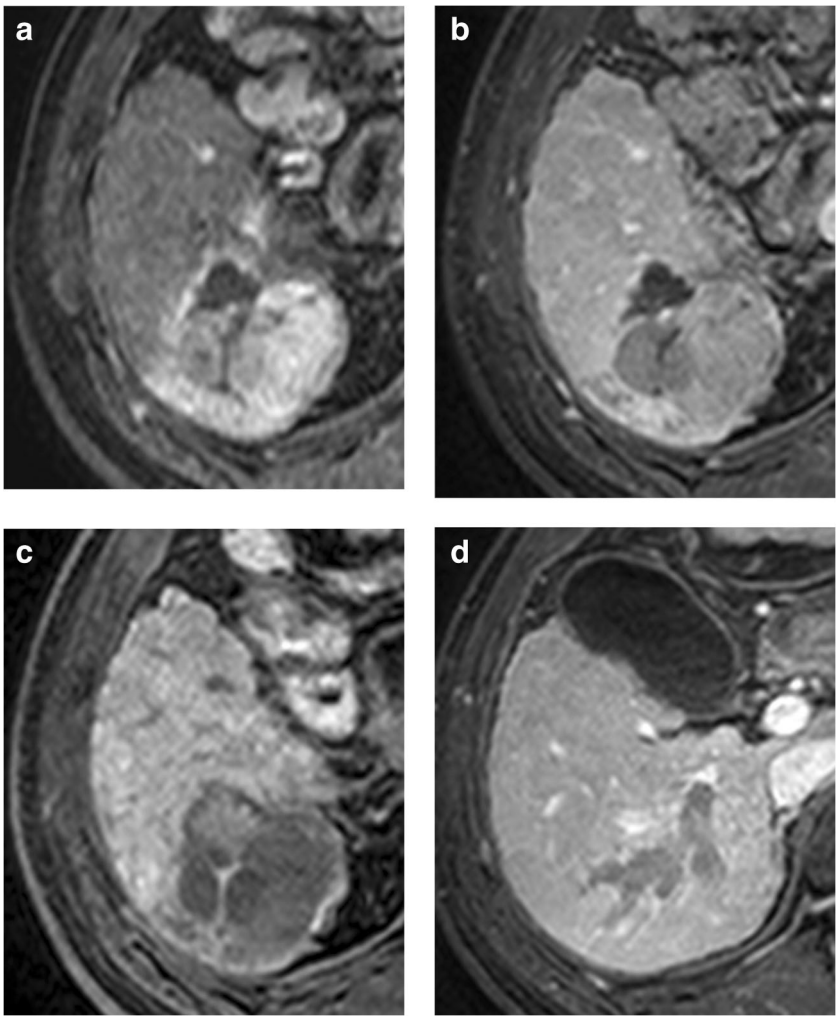

Fig. 5 A 4.2-cm sarcomatoid hepatocellular carcinoma of LR-TIV category in a 47-year-old man. Axial T1-weighted images acquired during the arterial (**a**) and portal venous (**b**) phases show a subtle lobulated mass with wash-in and washout enhancement patterns. **c** Axial hepatobiliary phase image shows heterogeneous hypointensity of the mass with mosaic appearance. Therefore, this mass shows MR findings that are consistent with LR-5. **d** Portal phase image shows diffuse tumor thrombosis along the portal veins

SCs [9–12] (e.g., large necrosis area, and frequent intrahepatic and extrahepatic metastases) were not significantly different between SCs and iCCAs. Although targetoid appearance or capsular retraction was less common in SCs than in iCCAs, differentiating SCs from iCCAs before histologic confirmation seems difficult.

This study has several limitations. First, the retrospective design imposes an inevitable selection bias. In particular, the selection of patients with HCC or iCCA using propensity score matching could not reflect actual disease prevalence. However, we chose this method because the incidence of SCs was much lower than that of HCCs or

Table 2 Diagnostic performance of the LI-RADS in high-risk patients

	LR-5/5V			LR-M/MV		
	Sensitivity	Specificity	Accuracy	Sensitivity	Specificity	Accuracy
All ($n = 123$)	82.4 (56/68)	85.5 (47/55)	83.7 (103/123)	81.8 (45/55)	85.3 (58/68)	83.7 (103/123)
SC ($n = 33$)	NA*	84.8 (28/33)	NA*	78.8 (26/33)	NA†	NA†
HCC ($n = 68$)	82.4 (56/68)	NA†	NA†	NA*	85.3 (58/68)	NA*
iCCA ($n = 22$)	NA*	86.4 (19/22)	NA*	86.4 (19/22)	NA†	NA†

In LR-5/5V, the sensitivity, specificity, and accuracy were calculated for the diagnosis of HCC. In LR-M/MV, those were calculated for the diagnosis of non-HCC malignancy. *LI-RADS*, Liver Imaging Reporting and Data System; *SC*, sarcomatoid carcinoma; *HCC*, hepatocellular carcinoma; *iCCA*, intrahepatic cholangiocarcinoma; *NA*, not applicable

*These values could not be calculated due to no disease-positive patients in each group

† These values could not be calculated due to no disease-negative patients in each group

Table 3 Differences in the clinical and MRI features between SCs, HCCs, and iCCAs

	HCC (n = 92)	SC (n = 46)	iCCA (n = 46)	*p*-value*	*p*-values of post-hoc test†		
					SC vs. HCC	SC vs. iCCA	HCC vs. iCCA
Clinical features							
Age (years)	61.3 ± 10.6	60.0 ± 10.0	62.2 ± 10.9	0.563			
Sex				0.180			
Male	75 (81.5)	35 (76.1)	31 (67.4)				
Female	17 (18.5)	11 (23.9)	15 (32.6)				
CLD				0.006	> 0.999	0.057	0.006
No	24 (26.1)	13 (28.3)	24 (52.2)				
Yes	68 (73.9)	33 (71.7)	22 (47.8)				
Histologic confirmation				0.261			
Operation	44 (47.8)	28 (60.9)	27 (58.7)				
Biopsy	48 (52.2)	18 (46.2)	19 (41.3)				
MRI features							
Size (cm)	3.8 (1.5, 20)	4.8 (1, 20.6)	5.2 (1.5, 13.3)	0.172			
Shape				< 0.001	0.009	> 0.999	< 0.001
Round	42 (45.7)	8 (17.4)	3 (6.5)				
Lobulated	35 (38.0)	23 (50.5)	32 (69.6)				
Irregular/geographic	15 (16.3)	15 (32.6)	11 (23.9)				
APHE				< 0.001	< 0.001	> 0.999	< 0.001
No	1 (1.1)	3 (6.5)	4 (8.7)				
Rim-like	5 (5.4)	30 (65.2)	32 (69.6)				
Non-rim like	86 (93.5)	13 (28.3)	10 (21.7)				
Washout				< 0.001	< 0.001	0.685	< 0.001
No	14 (15.2)	29 (63.0)	30 (65.2)				
Peripheral	0 (0)	3 (6.5)	10 (21.7)				
Non-peripheral	78 (84.8)	14 (30.4)	6 (13.0)				
Delayed central enhancement				< 0.001	0.030	0.192	< 0.001
No	88 (95.7)	37 (80.4)	29 (63.0)				
Yes	4 (4.3)	9 (19.6)	17 (37.0)				
Enhancing capsule				< 0.001	< 0.001	0.474	< 0.001
No	46 (50.0)	39 (84.8)	44 (95.7)				
Yes	46 (50.0)	7 (15.2)	2 (4.3)				
Nonenhancing capsule				0.008	0.021	> 0.999	0.057
No	73 (79.3)	44 (95.7)	43 (93.5)				
Yes	19 (20.7)	2 (4.3)	3 (6.5)				
T2WI				0.853			
Hypo	1 (1.1)	0 (0)	0 (0)				
Iso	3 (3.3)	2 (4.3)	1 (2.2)				
Hyper	88 (95.7)	44 (95.7)	45 (97.8)				
Bright T2WI				0.058			
No	58 (63.0)	29 (63.0)	21 (45.7)				
Small	32 (34.8)	15 (32.6)	19 (41.3)				
Large	2 (2.2)	2 (4.3)	6 (13.0)				
DWI restriction				0.457			
No	3 (3.4)	1 (2.3)	0 (0)				
Yes	85 (96.6)	43 (97.7)	45 (100)				

Table 3 (continued)

	HCC (n = 92)	SC (n = 46)	iCCA (n = 46)	*p*-value*	*p*-values of post-hoc test†		
					SC vs. HCC	SC vs. iCCA	HCC vs. iCCA
‡Target sign on DWI				<0.001	0.021	<0.001	<0.001
No	81 (92.0)	33 (75.0)	16 (35.6)				
Yes	7 (8.0)	11 (25.0)	29 (64.4)				
HBP SI				0.482			
Hypo	48 (98.0)	33 (100)	38 (100)				
Iso	0 (0)	0 (0)	0 (0)				
Hyper	1 (2.0)	0 (0)	0 (0)				
‡Target sign on HBP				<0.001	0.018	0.003	<0.001
No	48 (98.0)	26 (78.8)	15 (39.5)				
Yes	1 (2.0)	7 (21.2)	23 (60.5)				
Tumor in vein				0.928			
No	80 (87.0)	41 (89.1)	40 (87.0)				
Yes	12 (13.0)	5 (10.9)	6 13.0)				
Fat				<0.001	0.051	0.351	<0.001
No	68 (73.9)	42 (91.3)	46 (100)				
Yes	24 (26.1)	4 (8.7)	0 (0)				
Blood				0.324			
No	70 (76.1)	36 (78.3)	40 (87.0)				
Yes	22 (19.0)	10 (21.7)	6 (13.0)				
Mosaic appearance				0.001	0.027	>0.999	0.009
No	72 (78.3)	44 (95.7)	45 (97.8)				
Yes	20 (21.7)	2 (4.3)	1 (2.2)				
Capsular retraction				<0.001	>0.999	0.009	<0.001
No	89 (96.7)	43 (93.5)	32 (69.6)				
Yes	3 (3.3)	3 (6.5)	14 (30.4)				
Biliary dilatation				<0.001	<0.001	0.585	<0.001
No	87 (94.6)	32 (69.6)	26 (56.5)				
Yes	5 (5.4)	14 (30.4)	20 (43.5)				
Intrahepatic metastasis				0.187			
No	66 (71.7)	26 (56.5)	29 (63.0)				
Yes	26 (28.3)	20 (43.5)	17 (37.0)				
Extrahepatic metastasis				<0.001	0.009	>0.999	0.048
No	76 (82.6)	25 (54.3)	26 (56.5)				
Yes	16 (17.4)	21 (45.7)	20 (43.5)				

Data in parentheses are percentages except tumor size (median and range)

MRI, magnetic resonance imaging; *SC*, sarcomatoid carcinoma; *HCC*, hepatocellular carcinoma; *iCCA*, intrahepatic cholangiocarcinoma; *CLD*, chronic liver disease; *APHE,* arterial phase hyperenhancement; *WI,* wash-in; *WO*, washout; *DWI,* diffusion-weighted imaging; *HBP,* hepatobiliary phase

* *p*-values from the comparison among SCs, HCCs, and iCCAs by using one-way analysis of variance

† Adjusted *p*-values using Bonferroni correction

‡ Diffusion-weighted imaging (DWI) and hepatobiliary phase (HBP) were unavailable in 7 and 64 patients, respectively

Table 4 Sarcomatoid carcinomas: comparison between LR-M/MV and LR-4/5/5V in high-risk patients

	LR-M/MV ($n = 26$)	LR-4/5/5 V ($n = 7$)	p value
Clinical features			
Age (years)	59.6 ± 8.5	50.9 ± 7.9	0.020
Sex			0.093
Male	23 (88.5)	4 (57.1)	
Female	3 (11.5)	3 (42.9)	
Histologic confirmation			> 0.999
Operation	20 (76.9)	6 (85.7)	
Biopsy	6 (23.1)	1 (14.3)	
Subtype of SC			0.274
S-HCC	11 (42.3)	5 (71.4)	
S-iCCA	7 (26.9)	0 (0)	
S-cHCC-CC	5 (19.2)	2 (28.6)	
u-SC	3 (11.5)	0 (0)	
MRI features			
Size (cm)	4.3 (1.3, 20.6)	1.9 (1.0, 4.2)	0.012
Shape			0.032
Round	3 (11.5)	4 (57.1)	
Lobulated	15 (57.7)	2 (28.6)	
Irregular/geographic	8 (30.8)	1 (14.3)	
APHE			< 0.001
No	1 (3.8)	0 (0)	
Rim-like	23 (88.5)	0 (0)	
Non-rim like	2 (7.7)	7 (100)	
Washout			< 0.001
No	19 (73.1)	0 (0)	
Peripheral	3 (11.5)	0 (0)	
Non-peripheral	4 (15.4)	7 (100)	
Delayed central enhancement			0.301
No	20 (76.9)	7 (100)	
Yes	6 (23.1)	0 (0)	
Enhancing capsule			0.011
No	24 (92.3)	3 (42.9)	
Yes	2 (7.7)	4 (57.1)	
Nonenhancing capsule			0.384
No	25 (96.2)	6 (85.7)	
Yes	1 (3.8)	1 (14.3)	
T2WI			>0.999
Hypo	0 (0)	0 (0)	
Iso	2 (7.7)	0 (0)	
Hyper	24 (92.3)	7 (100)	
Bright T2WI			>0.999
No	17 (65.4)	5 (71.4)	
Small	9 (34.6)	2 (28.6)	
Large	0	0	
DWI restriction			> 0.999
No	1 (4.2)	0 (0)	
Yes	23 (95.8)	7 (100)	
Target sign on DWI‡			0.146
No	16 (66.7)	7 (100)	
Yes	8 (33.3)	0 (0)	
HBP SI			> 0.999
Hypo	20 (100)	5 (100)	
Iso	0 (0)	0 (0)	
Hyper	0 (0)	0 (0)	
Target sign on HBP‡			0.289
No	14 (70.0)	5 (100)	
Yes	6 (30.0)	0 (0)	
Tumor in vein			0.523
No	24 (92.3)	6 (85.7)	
Yes	2 (7.7)	1 (14.3)	
Fat			0.555
No	22 (84.6)	7 (100)	
Yes	4 (15.4)	0 (0)	
Blood			> 0.999
No	22 (84.6)	6 (85.7)	
Yes	4 (15.4)	1 (14.3)	
Mosaic appearance			0.040
No	26 (100)	5 (71.4)	
Yes	0 (0)	2 (28.6)	
Capsular retraction			> 0.999
No	26 (100)	7 (100)	
Yes	0 (0)	0 (0)	
Biliary dilatation			0.555
No	22 (84.6)	7 (100)	
Yes	4 (15.4)	0 (0)	
Intrahepatic metastasis			0.032
No	14 (53.8)	7 (100)	
Yes	12 (46.2)	0 (0)	
Extrahepatic metastasis			> 0.999
No	22 (84.6)	5 (71.4)	
Yes	4 (15.4)	2 (28.6)	

Data in parentheses are percentages except tumor size (median and range)

CLD, chronic liver disease; *SC*, sarcomatoid carcinoma; *S-HCC*, sarcomatoid hepatocellular carcinoma; *S-iCCA*, sarcomatoid intrahepatic cholangiocarcinoma; *S-cHCC-CC*, sarcomatoid combined hepatocellular and cholangiocarcinoma; *u-SC*, undifferentiated sarcomatoid carcinoma; *MRI*, magnetic resonance imaging; *APHE*, arterial-phase hyperenhancement; *WI*, wash-in; *WO*, washout

‡ Diffusion-weighted imaging (DWI) and hepatobiliary phase (HBP) were unavailable in 2 and 8 patients, respectively

iCCAs. Second, the analyzed MRI features of each hepatic malignancy might be biased, because we matched the histologic confirmation method during the selection process of HCC and iCCA. Biopsy-confirmed hepatic tumors would be larger and more likely inoperable. Although the mean sizes of SCs, HCCs, and iCCAs were approximately 5 cm without significant difference, they could not reflect their actual size distribution. Nevertheless, comparing the MRI findings of similar-sized SCs, HCCs, and iCCAs could be beneficial. Third, as the study population was recruited over a long study period, MRI hardware, contrast materials, and scanning parameters were inhomogeneous. However, we believe that the significant results in our study could be assessable regardless of the examination protocol; hence, it can be generalized in different studies. Fourth, a test bolus technique with gadoxetate disodium used in some patients might affect the assessment of "washout" on portal venous phase. Finally, the small number of patients with SC may limit subgroup analyses. Moreover, the small number of patients with SCs categorized as LR-4/5/5V compared with those categorized as LR-M/MV might lessen the power to detect differences of clinical and MRI features between two groups. However, to our knowledge, this is the largest study on hepatic SCs evaluating the MRI findings.

In conclusion, our study showed that most SCs can be classified as LR-M on MRI by using the LI-RADS v2017, but small lesions may be indistinguishable from HCCs. Our results suggest that the use of LI-RADS can be helpful to lead to a correct diagnosis of sarcomatoid carcinoma before treatment.

Acknowledgements The authors thank Ha Yan Kim for her help with the statistical advice.

Funding The authors state that this work has not received any funding.

Compliance with ethical standards

Guarantor The scientific guarantor of this publication is Myeong-Jin Kim.

Conflict of interest The authors of this manuscript declare no relationships with any companies whose products or services may be related to the subject matter of the article.

Statistics and biometry Nieun Seo performed statistical analysis, who is one of the coauthors. Ha Yan Kim, Ph.D., who is a member of our biostatistics collaboration unit, Yonsei University College of Medicine, gave us advice on the statistical analysis.

Informed consent Written informed consent was waived by the Institutional Review Board for this retrospective case-control study.

Ethical approval Institutional Review Board approval was obtained.

Methodology
- retrospective
- diagnostic or prognostic study
- performed at one institution

References

1. Kakizoe S, Kojiro M, Nakashima T (1987) Hepatocellular carcinoma with sarcomatous change. Clinicopathologic and immunohistochemical studies of 14 autopsy cases. Cancer 59:310–316
2. Giunchi F, Vasuri F, Baldin P, Rosini F, Corti B, D'Errico-Grigioni A (2013) Primary liver sarcomatous carcinoma: report of two cases and review of the literature. Pathol Res Pract 209:249–254
3. Fred TB, Fatima C, Ralph HH, Neil DT (2010) WHO classification of tumours of the digestive system. IARC press, Lyon
4. Nishi H, Taguchi K, Asayama Y et al (2003) Sarcomatous hepatocellular carcinoma: a special reference to ordinary hepatocellular carcinoma. J Gastroenterol Hepatol 18:415–423
5. Hwang S, Lee SG, Lee YJ et al (2008) Prognostic impact of sarcomatous change of hepatocellular carcinoma in patients undergoing liver resection and liver transplantation. J Gastrointest Surg 12:718–724
6. Kaibori M, Kawaguchi Y, Yokoigawa N et al (2003) Intrahepatic sarcomatoid cholangiocarcinoma. J Gastroenterol 38:1097–1101
7. Lu J, Xiong XZ, Li FY et al (2015) Prognostic significance of sarcomatous change in patients with hepatocellular carcinoma after surgical resection. Ann Surg Oncol 22(Suppl 3):S1048–S1056
8. Liao SH, Su TH, Jeng YM et al (2018) Clinical manifestations and outcomes of patients with sarcomatoid hepatocellular carcinoma. Hepatology. https://doi.org/10.1002/hep.30162
9. Gu KW, Kim YK, Min JH, Ha SY, Jeong WK (2017) Imaging features of hepatic sarcomatous carcinoma on computed tomography and gadoxetic acid-enhanced magnetic resonance imaging. Abdom Radiol (NY) 42:1424–1433
10. Koo HR, Park MS, Kim MJ et al (2008) Radiological and clinical features of sarcomatoid hepatocellular carcinoma in 11 cases. J Comput Assist Tomogr 32:745–749
11. Honda H, Hayashi T, Yoshida K et al (1996) Hepatocellular carcinoma with sarcomatous change: characteristic findings of two-phased incremental CT. Abdom Imaging 21:37–40
12. Bilgin M, Toprak H, Bilgin SS, Kondakci M, Balci C (2012) CT and MRI findings of sarcomatoid cholangiocarcinoma. Cancer Imaging 12:447–451
13. Chung YE, Park MS, Park YN et al (2009) Hepatocellular carcinoma variants: radiologic-pathologic correlation. AJR Am J Roentgenol 193:W7–W13
14. Shi D, Ma L, Zhao D et al (2018) Imaging and clinical features of primary hepatic sarcomatous carcinoma. Cancer Imaging 18:36
15. American College of Radiology. Liver imaging reporting and data system (LI-RADS). American College of Radiology. Web site. https://www.acr.org/Clinical-Resources/Reporting-and-Data-Systems/LI-RADS/CT-MRI-LI-RADS-v2017. Accessed June 1, 2017
16. Heimbach JK, Kulik LM, Finn RS et al (2018) AASLD guidelines for the treatment of hepatocellular carcinoma. Hepatology 67:358–380
17. European Association for the Study of the Liver (2018) EASL clinical practice guidelines: management of hepatocellular carcinoma. J Hepatol 69:182–236
18. Mitchell DG, Bruix J, Sherman M, Sirlin CB (2015) LI-RADS (liver imaging reporting and data system): summary, discussion, and consensus of the LI-RADS management working group and future directions. Hepatology 61:1056–1065
19. An C, Rhee H, Han K et al (2017) Added value of smooth hypointense rim in the hepatobiliary phase of gadoxetic acid-enhanced MRI in identifying tumour capsule and diagnosing hepatocellular carcinoma. Eur Radiol 27:2610–2618
20. Seo N, Kim DY, Choi JY (2017) Cross-sectional imaging of intrahepatic cholangiocarcinoma: development, growth, spread, and prognosis. AJR Am J Roentgenol 209:W64–w75
21. Ariizumi S, Kotera Y, Takahashi Y et al (2011) Mass-forming intrahepatic cholangiocarcinoma with marked enhancement on arterial-phase computed tomography reflects favorable surgical outcomes. J Surg Oncol 104:130–139
22. Kim SJ, Lee JM, Han JK, Kim KH, Lee JY, Choi BI (2007) Peripheral mass-forming cholangiocarcinoma in cirrhotic liver. AJR Am J Roentgenol 189:1428–1434
23. Joo I, Lee JM, Lee SM, Lee JS, Park JY, Han JK (2016) Diagnostic accuracy of liver imaging reporting and data system (LI-RADS) v2014 for intrahepatic mass-forming cholangiocarcinomas in patients with chronic liver disease on gadoxetic acid-enhanced MRI. J Magn Reson Imaging 44:1330–1338
24. Kim YY, An C, Kim S, Kim MJ (2018) Diagnostic accuracy of prospective application of the liver imaging reporting and data system (LI-RADS) in gadoxetate-enhanced MRI. Eur Radiol 28:2038–2046
25. Fraum TJ, Tsai R, Rohe E et al (2018) Differentiation of hepatocellular carcinoma from other hepatic malignancies in patients at risk: diagnostic performance of the liver imaging reporting and data system version 2014. Radiology 286:158–172